

Locating scatterers by non-physical scattered waves obtained by seismic interferometry

Harmankaya, U., Kaslilar, A., Thorbecke, J., Wapenaar, K., and Draganov, D.

Abstract

The investigation and detection of near-surface structures (such as cavities, caves, sinkholes, tunnels, mineshafts, buried objects, archeological ruins, water reservoir, etc.) is important to mitigate geo- and environmental hazards. In a former study, we suggested a method based on active-source seismic interferometry for locating the scatterers and we showed the applicability of the method in a simple model. In our method, we use only one source at the surface and non-physical scattered waves retrieved by seismic interferometry to estimate the location of the scatterer. In this paper, we show the effectiveness of the method in case of lateral variations. We use both scattered body and surface waves to estimate the location of a corner diffractor and a scatterer, respectively, and we obtain very good estimations. The method is promising for near-surface seismic field applications.

Introduction

We use non-physical scattered body and surface waves retrieved by seismic interferometry (SI) to estimate the location of a corner diffractor and a near-surface scatterer (such as cavity, cave, tunnel, mineshaft, buried object, etc.), respectively. For our method we use active source SI and only one source at the surface (Harmankaya et al., 2012). As we use only one source, it is very unlikely that the source is at the stationary point for retrieving physical scattered waves. To obtain the complete Green's function between the receivers whose recorded responses we cross-correlate, the boundary sources (primary or secondary) need to effectively enclose these receivers (Wapenaar and Fokkema, 2006). When the receivers are not equally illuminated from all directions by the boundary sources, non-physical arrivals (ghosts) will appear in the SI result (Snieder et al., 2006; Halliday and Curtis, 2009; Halliday et al., 2010). Because SI effectively redatum sources from places away from the scatterers to the target area, the unwanted extra effects, due to propagation from the active-source locations through possibly laterally changing medium to the receivers close to the target area, are eliminated and non-physical ghost scattered waves are retrieved. We perform 2D elastic finite-difference modelling (Thorbecke and Draganov, 2011) and show the effectiveness of our method in the presence of lateral inhomogeneities. We obtain very good estimations of the subsurface location of a corner diffractor and a scatterer by using non-physical scattered S-waves and Rayleigh waves, respectively.

Method

In this study, we use non-physical scattered body and surface waves, obtained from SI, and inversion to estimate the location of a diffractor or scatterer (Harmankaya et al., 2012). SI is applied to the scattered wavefield obtained from the seismic records of the original geometry by using only one source and by cross-correlating the reference trace d^{VS} (the trace at the virtual-source position) with the rest of the traces, d^i , which are present on the seismic record. This relation is

$$C_{d^i d^{VS}}(\tau) = \sum_n d^i(t_n) d^{VS}(t_n + \tau). \quad (1)$$

Application of Eq. (1) will eliminate the common travel-path from the source to the scatterer and will result in the retrieval of a non-physical ghost scattered body or surface waves.

To estimate the location of the diffractor or scatterer, the following theoretical ghost travel-time relation is used,

$$t = \frac{1}{V} \left\{ \left[(x_i^r - x)^2 + (z_i^r - z)^2 \right]^{1/2} - \left[(x_{vs} - x)^2 + (z_{vs} - z)^2 \right]^{1/2} \right\}. \quad (2)$$

The relation gives the retrieved ghost traveltimes between the virtual source, the scatterer and the receivers. In Eq. (2), V is the wave velocity, i is the index for the receiver numbers, vs denote the virtual source and x and z are the locations of the scatterer in the horizontal and vertical direction, respectively.

To find the location of the object, the traveltime relation (Eq. 2) and the traveltimes obtained for each virtual source location are used in the inversion. The nonlinear problem is solved iteratively. The system of equations for the forward problem is denoted as $\Delta \mathbf{d} = \mathbf{G} \Delta \mathbf{m}$. The difference between the observed t_{obs} (retrieved), and the calculated t_{calc} ghost scattered data is denoted by $\Delta \mathbf{d} = t_{obs} - t_{calc}$, the unknown model parameters - the x and z location of the object - are denoted by the vector $\Delta \mathbf{m}$, while the Jacobian matrix is represented by \mathbf{G} . The damped least-squares solution of the inverse problem is given in terms of Singular Value Decomposition (SVD) as

$$\Delta \mathbf{m} = \mathbf{V} \mathbf{\Lambda} (\mathbf{\Lambda}^2 + \beta^2 \mathbf{I})^{-1} \mathbf{U}^T \Delta \mathbf{d}, \quad (3)$$

where \mathbf{V} , $\mathbf{\Lambda}$, \mathbf{U} , \mathbf{I} and β are the model-space eigenvectors, the diagonal matrix containing the eigenvalues, the data-space eigenvectors, the identity matrix and the damping parameter, respectively.

Considering Eq. (3), the inverse problem is solved to find the location of the object. The uncertainties of the estimations are calculated by the model covariance matrix given as

$$\text{cov}[\mathbf{m}] = \sigma^2 \mathbf{V} \mathbf{\Lambda}^2 (\mathbf{\Lambda}^2 + \beta^2 \mathbf{I})^{-1} \mathbf{V}^T \quad (4)$$

where σ^2 is

$$\sigma^2 = \frac{1}{n - n_m} \sum_{i=1}^n (t_{\text{obs}} - t_{\text{calc}})^2. \quad (5)$$

Here, n is the number of observed data, and n_m is the number of model parameters (here $n_m = 2$). In the following examples, the uncertainties of the estimated parameters are calculated with 95 % confidence (1.96σ) and plotted with estimated model parameters for each selected virtual source.

Estimation of the Location of the Objects by the Interferometric Ghosts of the Scattered Waves

To show the effectiveness of the method in the presence of lateral inhomogeneities, the geometry and the medium parameters of the model given in Figure 1 are considered.

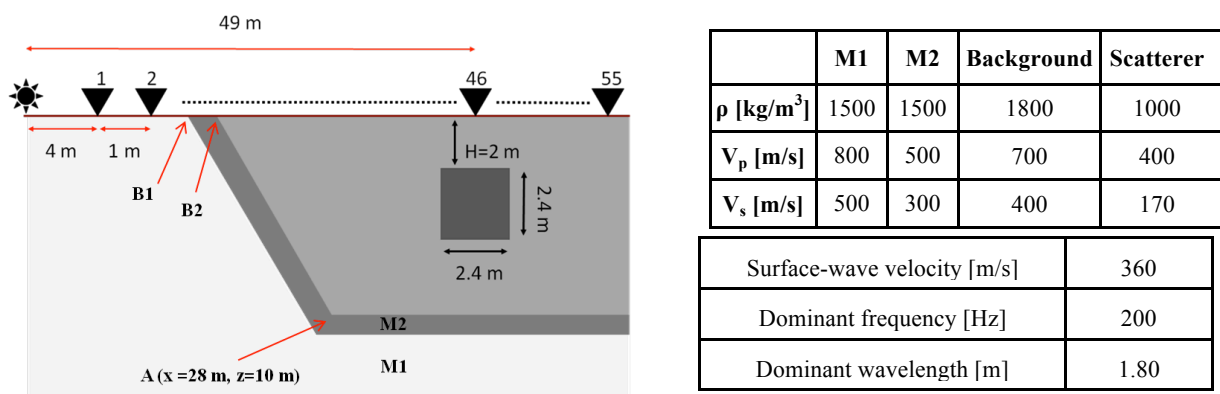


Figure 1 Schematic view of the scale model (left): the source (star), receivers (triangles) and scatterer (grey square). A represents the corner of the low-velocity zone; B1 and B2 represent the two interfaces between the source and the receivers. M1 and M2 represent the media having different velocities. The modelling parameters are given in the table (right).

The 2D finite difference modelling program of Thorbecke and Draganov (2011) is used and the wavefield shown in Figure 2a is calculated. It should be noted that the starting point of the coordinate system is arbitrarily chosen and it is at the position of the actual source. Here, we try to estimate both the location of the scatterer (Figure 1 grey square) from scattered surface waves (Figure 2a Rsc), and the location of the diffractor (A in Figure 1) from scattered S-wave (A in Figure 2a).

To obtain the scattered wavefield, an f - k filter is used, which removed most of the direct Rayleigh waves and direct and refracted P-waves (Figure 2b). SI is applied to the extracted scattered waves by using Eq. (1). In Figure 2c-e the retrieved ghost scattered surface waves for virtual-source locations at receivers 26, 46 and 55 (29, 49 and 58 m) are given, respectively. The ghost traveltimes are picked from the maximum amplitude of the retrieved ghost scattered surface waves (red curves on Figure 2c-e). To find the location of the scatterer, the traveltime relation (Eq. 2) and the traveltimes obtained for each virtual-source location (red curves in Figure 2c-e) are used in the inversion (Eq. 3). The velocities are considered as known parameters in the inversion and they are estimated from the shot records. The observed and the calculated traveltimes of the ghost scattered surface waves are plotted in Figure 3a for each virtual source location. The initial and the updated model parameters for each iteration are given in Figure 3b. After eight iterations, the model parameters - the horizontal and vertical location of the scatterer - get closer to the actual values. The uncertainties in the model parameters are calculated by Eqs. (4-5) and the results are plotted in Figure 3c for each virtual-source location and their average values. The blue lines in Figure 3c denote the midpoint, the upper and

lower bounds of the scatterer. The estimated locations are within the size of the scatterer and it can be concluded that the location of the scatterer is well estimated.

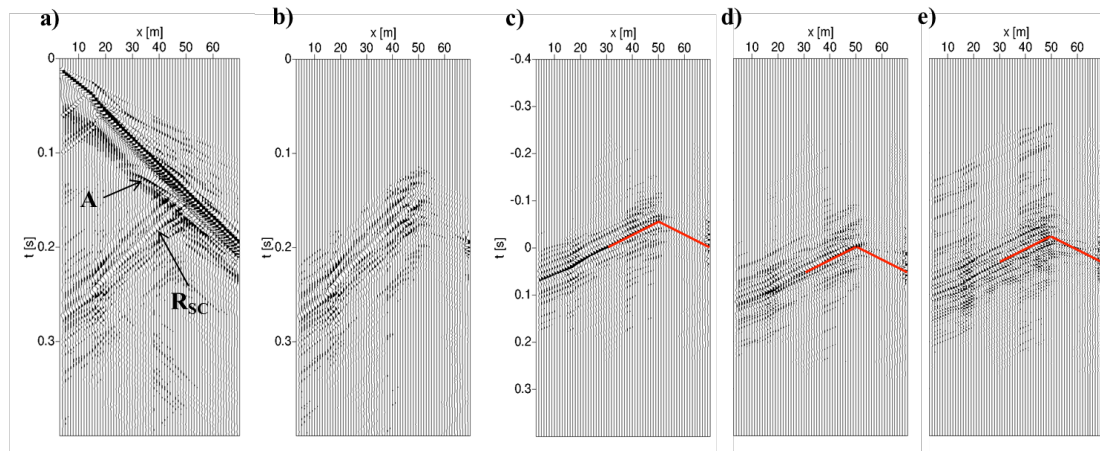


Figure 2 (a) Shot gather obtained by finite-difference modelling. (b) The scattered wavefield. (c), (d) and (e): ghost scattered surface waves retrieved by applying SI to (b) for virtual-source locations at receivers 26, 46 and 55 (29, 49 and 58 m), respectively. A: scattered S-wave and Rsc:scattered Rayleigh wave.

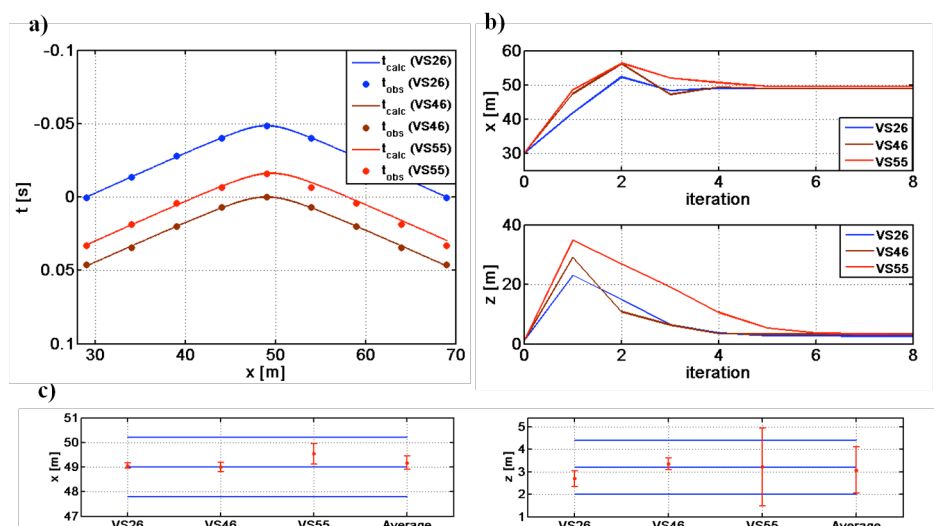


Figure 3 (a) Observed and calculated travel times, related to the square scatterer in Figure 1, (b) estimated horizontal and vertical locations of the scatterer for the virtual sources 26 (blue, 29 m), 46 (brown, 49 m) and 55 (red, 58 m). (c) Estimated model parameters and their 95% confidence limits, blue lines show the actual midpoint and the upper and lower bounds of the scatterer.

To find the location of the corner diffractor, the scattered S-wave (A in Figure 2a) is used. The arrivals other than the scattered S-wave are filtered and muted out (due to limited space, not shown here). The remaining S-wave scattered field is used in the SI procedure described before. For this example the virtual sources 26, 30 and 34 (29, 33 and 37 m) are considered. The best fit between the observed and calculated traveltimes, the estimated model parameters for each iteration and their uncertainties are given in Figure 4 a, b and c, respectively. It is observed that the location of the diffractor is well estimated.

Conclusion

The method proposed for obtaining the location of a near-surface scatterer by using traveltimes of non-physical (ghost) scattered body and surface waves is applied to a laterally inhomogeneous model

to show the effectiveness of the method. By considering only one surface source, the ghost traveltimes of scattered waves retrieved from SI are used in the inversion to find the location of the scatterer. Very good estimation of the location of the diffractor and the scatterer is obtained.

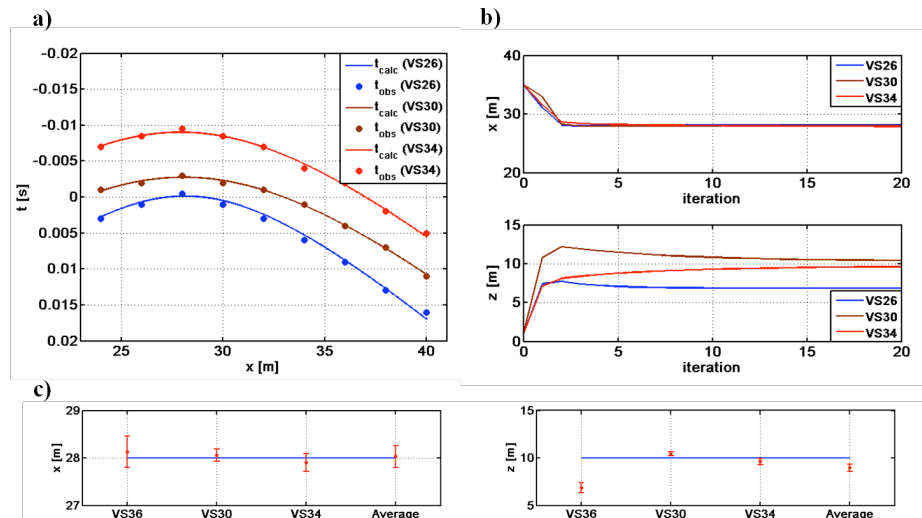


Figure 4 (a) Observed and calculated travel times, related to the corner diffractor at *A* in Figure 1, (b) estimated horizontal and vertical locations of the scatterer for the virtual sources 26 (blue, 29 m), 30 (brown, 33 m) and 34 (red, 37 m). (c) Estimated model parameters and their 95% confidence limits, blue line shows the actual position of the corner diffractor.

Acknowledgements

This work is supported by **TUBITAK (The Scientific and Technological Research Council of Turkey)** with the project **110Y250** titled “**Detecting Near-surface Scatterers by Inverse Scattering and Seismic Interferometry of Scattered Surface Waves**”. We gratefully acknowledge this financial support. The research of D.D. is supported by the Division for Earth and Life Sciences (ALW) with financial aid from the Netherlands Organization for Scientific Research (NWO). We also thank the Colorado School of Mines for providing the Seismic Un*x (Cohen and Stockwell, 2012) package as open source software.

References

- Cohen, J.K., Stockwell, Jr.J.W., [2012] CWP/SU: Seismic Un*x Release No. 43: an open source software package for seismic research and processing. Center for Wave Phenomena, Colorado School of Mines.
- Halliday, D. F., Curtis, A., [2009] Seismic interferometry of scattered surface waves in attenuative media. *Geophys. J. Int.* **185**, 419-446.
- Halliday, D. F., Curtis, A., Vermeer, P., Strobbia, C., Glushchenko, A., van Manen, D.J., Robertsson, J.O.A., [2010] Interferometric ground-roll removal: Attenuation of scattered surface waves in single-sensor data. *Geophysics* **75** (2), A15-A25.
- Harmankaya, U., Kaslilar, A., Thorbecke, J., Wapenaar K., Draganov, D., [2012] Estimating the location of scatterers by seismic interferometry of scattered surface waves. Extended Abstracts of the 74th EAGE Meeting, Copenhagen. X008.
- Snieder, R., Wapenaar, K., Larner, K., [2006] Spurious multiples in seismic interferometry of primaries. *Geophysics* **71**, SI111–SI124.
- Thorbecke, J., Draganov, D., [2011] Finite-difference modeling experiments for seismic interferometry. *Geophysics* **75**, H1-H18.
- Wapenaar, K., Fokkema, J., [2006] Green’s function representations for seismic interferometry. *Geophysics* **71** (4), SI33-SI46.